

# Voltage Restoration in Microgrids using Temporal Logic Specifications

Fatima Z. Taousser<sup>\*</sup>, Mohammed M. Olama<sup>†</sup>, Seddik M. Djouadi<sup>\*</sup>, Yichen Zhang<sup>‡</sup>, Yaosuo Xue<sup>§</sup>, Ben Ollis<sup>§</sup>, and Kevin Tomsovic<sup>\*</sup>

<sup>\*</sup>Department of Electrical Engineering and Computer Science, University of Tennessee, Knoxville, TN 37996

Email: {ftaousse, mdjouadi, tomsovic}@utk.edu

<sup>†</sup>Computational Sciences and Engineering Division, Oak Ridge National Laboratory, Oak Ridge, TN 37831

Email: olamahussem@ornl.gov

<sup>‡</sup>Energy System Division, Argonne National Laboratory, Lemont, IL 60439

Email: yichen.zhang@anl.gov

<sup>§</sup>Electrical and Electronics Systems Research Division, Oak Ridge National Laboratory, Oak Ridge, TN 37831

Email: {xuey, ollistb}@ornl.gov

**Abstract**—This paper proposes an energy storage controller synthesis method for voltage restoration in microgrids with respect to temporal logic specifications (TLSs). TLSs is introduced in this paper as a formalism to control the voltage variation of a critical bus against an operational bounds over time. The power system with synchronous generator (SG) connected to a critical load bus is modeled as a set of differential-algebraic equations and a simplified analytical model is derived to describe the voltage variation of this critical bus. The control objective is to schedule an optimal control input signal from a supportive energy storage system (ESS) connected to the critical bus, such that the voltage variation of the latter satisfies the TLSs, such as a finite-time restoration. The proposed control is verified on a lumped distribution system model. With this control diagram, supportive controllers can be designed to make voltage behaviors comply with grid codes and avoid unnecessary relay actions.

**Index Terms**—Voltage control, finite-time voltage restoration, numerical optimal control, temporal logic specification.

## I. INTRODUCTION

Microgrids are small scale power systems which represent one of the main building blocks of smart grids. In the event of disturbances, the primary control is applied to maintain the voltage and frequency stability [1], [2]. However, the primary control can lead to voltage and frequency deviations. To restore the voltage and frequency to their nominal values, secondary control is applied [1], [3]. In recent years, power systems have increasingly been utilizing diversified power resources for providing more reliable and efficient ancillary services [4], [5]. With the incorporation of renewable energy in the ancillary services, energy storage systems (ESSs) such as batteries and supercapacitors, serve as buffers for the power system to restore frequency and voltage to the allowable range [6]. The ESSs perform better than traditional generators and operating reserves with their quicker responsive capability; more precise control and capability to store and release energy in providing nearly net-zero energy services [7].

In electrical power systems, the voltage levels at all busses must be kept within permissible limits in order for the system to function properly, especially under intermittent renewable generations and constantly changing load demands. Unacceptable voltage variations may lead to system instability

and life-time degradation, or even damage to grid connected equipments. Many works have been applied to this area [8]–[11]. On the other hand, most specifications of power system control design are focused on set constraints [12]. However, voltage restoration has different temporal properties, since different ESSs have different response times. For this reason, the finite-time restoration of the voltage becomes a desired specification [8]. To avoid unnecessary relay actions and comply with grid codes, constraints of dwell time on specified sets need consideration. Motivated by that, we are interested in the secondary voltage control of a critical bus utilizing the support of the ESSs, by introducing the temporal logic specifications (TLSs).

TLSs are utilized to provide time-related specifications, such as after a fault occurs, the voltage at a critical bus should be restored to  $1 \text{ p.u} \pm 0.02 \text{ p.u}$  within 5 seconds. TLSs allow richer descriptions of specifications including set, logic, and time-related properties. The pioneering work in [13] introduces the TLSs for controller synthesis of energy storage systems, where a finite-time restoration is guaranteed. The work [14] derives a provable probabilistic guarantee in the stochastic environment of wind power generation. In [15], a numerical optimal control (NOC)-based control synthesis approach is proposed to schedule a controller for frequency support to satisfy the TLSs. The latter control synthesis approach has been introduced in [16], for the secondary voltage control design with TLSs, by considering that the critical bus is connected to an infinite bus.

This paper will investigate secondary voltage control with TLSs as in [16], but by considering that the critical bus is connected to a synchronous generator (SG). This represents an islanded microgrid case. During a disturbance, the voltage is required to be restored back within permissible limits at a required time, utilizing the support of the ESS. The controller will locally measure the voltage, estimate the size of disturbance, and compute the reactive power input to be injected from the ESS, such that, the voltage variation satisfies the TLSs constraint. The ESSs, which can meet voltage stability requirement in the form of TLSs, have more precise time-related performance measure, which can create economic benefits. Notice that, thus finite-time restoration and dwell time constraints are pressing and require a novel control approach.

This manuscript has been authored by UT-Battelle, LLC under Contract No. DE-AC05-00OR22725 with the U.S. Department of Energy.

## II. PRELIMINARIES ON TEMPORAL LOGIC SPECIFICATIONS

In this section, we briefly review the TLSs characteristics [17]. TLSs can be defined in terms of its syntax and semantics. Syntax describes the structure of syntactically formulas for the logic. Semantics describe the meaning of the formulas and the rules to evaluate them. The syntax of TLSs is defined as

$$\phi := \top, \varphi, \neg\phi, \phi_1 \wedge \phi_2, \phi_1 \vee \phi_2, \phi_1 \mathcal{U}_\tau \phi_2, \Rightarrow, \Leftrightarrow,$$

where  $\top$  denotes Boolean constant *True*.  $\neg$ ,  $\wedge$ ,  $\vee$ ,  $\Rightarrow$  and  $\Leftrightarrow$  are negation, conjunction, disjunction, implication and equivalence, respectively.  $\mathcal{U}_\tau$  is a temporal operator representing "until" and  $\tau$  is the time interval over  $\mathbb{R}_{\geq 0}$ .  $\varphi$  is a statement on the system variables that maps to the Boolean domain  $\mathbb{B} = \{\text{True}, \text{False}\}$ . A signal  $\xi$  satisfies the required TLS  $\varphi$  (i.e.,  $\xi \models \varphi$ ), if  $\varphi$  evaluates to *True* when  $\xi$  meets the conditions defined in  $\varphi$ . We can also derive two useful temporal operators:  $\xi \models \Diamond_{[t_1, t_2]} \varphi$  (eventually), where  $[t_1, t_2]$  is the time interval, if  $\varphi$  holds at some time step between  $t_1$  and  $t_2$ , and  $\xi \models \Box_{[t_1, t_2]} \varphi$  (always), if  $\varphi$  holds at every time step between  $t_1$  and  $t_2$ . Additionally, we define  $\varphi \mathcal{U}_{[t_1, t_2]} \psi$ , if  $\varphi$  holds at every time step before  $\psi$  holds and  $\psi$  holds at some time step between  $t_1$  and  $t_2$ . An example of a TLS is given as

$$\varphi = \Box \neg(x_1 > 10) \wedge \Box_{[2, 10]} (-2 < x_2 < 2),$$

which reads "x<sub>1</sub> is always less than 10, and x<sub>2</sub> is always bounded by -2 and 2 at each time step from 2s to 10s".

## III. VOLTAGE CONTROL WITH TEMPORAL LOGIC SPECIFICATION

### A. Problem Statement

This paper deals with the voltage control of a critical load bus. A lumped distribution system model is considered and it is shown with its equivalent circuit in Fig. 1 and Fig. 2, respectively. This system consists of a SG, which is equipped with a fast excitation system, connected through one transmission line to the load bus, which is considered as the critical bus, and it is connected to an ESS. The net load changes due to either the intermittency of renewable generation at the load side or abrupt demand change. The objective of the control strategy is to deliver reactive power from the ESS to maintain the voltage at the critical bus within permissible magnitude and time limits. This additional time constraint is generated by introducing some temporal logic specifications. The overall equations of the SG and the transmission line are presented.

The full state equations of the SG are given by [18],

$$\begin{aligned} \dot{\delta} &= \omega - \omega_s \\ \dot{\omega} &= \frac{\omega_s}{2H} [P_m - E_q I_q + (X_d - X'_d) I_d I_q + D(\omega - \omega_s)] \\ \dot{E}_q &= \frac{1}{T_{d0}} [E_q + (X_d - X'_d) I_d - E_{fd}] \\ \dot{E}_{fd} &= \frac{1}{T_A} (E_{fd} - \frac{K}{T_A} [V_{ref} - V_1]) \end{aligned} \quad (1)$$

satisfying the algebraic equations

$$\begin{aligned} V_d &= V_1 \sin(\delta - \theta_1) = X_q I_q, \\ V_q &= V_1 \cos(\delta - \theta_1) = E_q - X'_d I_d, \\ V_1 &= \sqrt{V_d^2 + V_q^2}, \end{aligned} \quad (2)$$

where,  $\delta, \omega, \omega_s, E_q, E_{fd}$  are the generator angle, frequency, synchronous frequency,  $q$ -axis transient voltage, and field voltage, respectively.  $\theta_1$  is the voltage phase angle at bus 1.  $I_d, I_q$  and  $V_d, V_q$  are the  $d$ -axis,  $q$ -axis currents and  $d$ -axis and  $q$ -axis voltages.  $X_d, X_q, X'_d$  are respectively the  $d$ -axis reactance,  $q$ -axis reactance, and  $d$ -axis transient reactance.

Suppose that the frequency is normalized as  $\omega_r = \frac{\omega}{\omega_s}$ . The linearized equations of the SG are given by

$$\begin{aligned} \Delta \dot{\delta} &= \omega_s \Delta \omega_r \\ \Delta \dot{\omega}_r &= \frac{1}{2H} [\Delta P_m - K_1 \Delta \delta - D \omega_s \Delta \omega_r - K_2 \Delta E_q] \\ \Delta \dot{E}_q &= \frac{1}{T_{d0}} [\frac{1}{K_3} \Delta E_q + K_4 \Delta \delta - \Delta E_{fd}] \\ \Delta \dot{E}_{fd} &= \frac{1}{T_A} [\Delta E_{fd} - K [\Delta V_{ref} - \Delta V_1]] \end{aligned} \quad (3)$$

$$\Delta V_1 = K_5 \Delta \delta + K_6 \Delta E_q, \quad (4)$$

where  $K_1 - K_6$  are the well-known linearization constants derived in [18].

Bus 2 is considered as the critical bus, the voltage of which is required to be controlled, satisfying a TLS constraint. An aggregated net load and an ESS are connected to the critical bus. The disturbance is considered as a load change and denoted by  $\Delta P_d$ . Assume the reactive power variation of the ESS under the control input, denoted by  $Q_c$ , is governed by the following state space model,

$$\dot{x} = Ax + Bu, \quad \Delta Q_c = Cx. \quad (5)$$

The power flow across the transmission line from the generator to bus 2, denoted by  $S_{12} = P_{12} + jQ_{12}$ , follows from Kirchhoff's laws as

$$S_{12} = V_1 \angle \theta_1 (I_{12}^*) = V_1 \angle \theta_1 \left( \frac{V_1 \angle \theta_1 - V_2 \angle \theta_2}{R_e + jX_e} \right)^*, \quad (6)$$

which leads to the following algebraic equations

$$\begin{aligned} P_{12} &= G_{12} V_1^2 + V_1 V_2 [G_{12} \cos(\theta_1 - \theta_2) + B_{12} \sin(\theta_1 - \theta_2)] \\ Q_{12} &= -B_{12} V_1^2 + V_1 V_2 [G_{12} \sin(\theta_1 - \theta_2) - G_{12} \cos(\theta_1 - \theta_2)], \end{aligned} \quad (7)$$

such that,

$$G_{12} + jB_{12} = \frac{R_e}{R_e^2 + X_e^2} - j \frac{X_e}{R_e^2 + X_e^2}, \quad (8)$$

where  $R_e$  and  $X_e$  are the external resistance and reactance, respectively. The linearized power flow in [19] is employed as follows

$$\begin{aligned} P_{12} &= G_{12} (V_1 - V_2) - B_{12} (\theta_1 - \theta_2) \\ Q_{12} &= -B_{12} (V_1 - V_2) - G_{12} (\theta_1 - \theta_2). \end{aligned} \quad (9)$$

Power balance at bus 2 can be expressed as

$$\begin{aligned} P_{12} &= P_L + \Delta P_d \\ Q_{12} &= Q_L - Q_c, \end{aligned} \quad (10)$$

such that  $P_L$  and  $Q_L$  are the active and reactive power of the load demand, respectively. Combining Eqs. (9) and (10) yields

$$P_L + \Delta P_d = G_{12} (V_1 - V_2) - B_{12} (\theta_1 - \theta_2) \quad (11)$$

$$Q_L - Q_c = -B_{12} (V_1 - V_2) - G_{12} (\theta_1 - \theta_2) \quad (12)$$

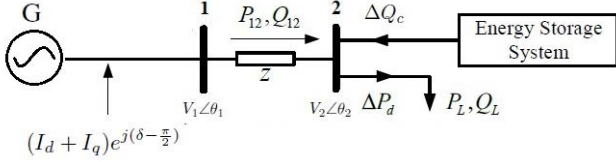


Fig. 1. A lumped distribution system model.

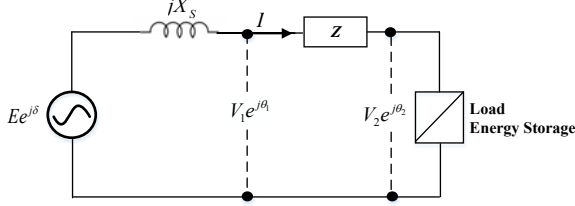


Fig. 2. Equivalent circuit.

One get, from (11)

$$\theta_1 - \theta_2 = \frac{-P_L - \Delta P_d + G_{12}(V_1 - V_2)}{B_{12}} \quad (13)$$

Substituting (13) into (12), we get the voltage at bus 2,

$$V_2 = C_1 Q_c + C_2 \Delta P_d + C_3 + V_1, \quad (14)$$

such that,

$$C_1 = \frac{-B_{12}}{G_{12}^2 + B_{12}^2}, \quad C_2 = \frac{-G_{12}}{G_{12}^2 + B_{12}^2}, \quad \text{and}$$

$$C_3 = \left( \frac{Q_L B_{12} - P_L G_{12}}{G_{12}^2 + B_{12}^2} \right).$$

So, the voltage deviation at bus 2 is described by

$$\Delta V_2 = C_1 \Delta Q_c + C_2 \Delta P_d + \Delta V_1, \quad (15)$$

and, therefore, it depends on the reactive power injected from the capacitor, the change in power load demand, and the voltage deviation at bus 1.

Substituting  $\Delta V_1$  and  $\Delta Q_c$  by there expressions (4) and (5), respectively, we get

$$\Delta V_2 = C_1 C x + C_2 \Delta P_d + K_5 \Delta \delta + K_6 \Delta E_q. \quad (16)$$

Consider the state space,

$$X = [\Delta \delta \quad \Delta \omega_r \quad \Delta E_q \quad \Delta E_{fd} \quad x]^T.$$

Based on (3), (5) and (16), the simplified model in state-space form can be expressed as follows

$$\begin{aligned} \dot{X} &= A'X + B'U \\ \Delta V_2 &= C'X + D'U, \end{aligned} \quad (17)$$

where

$$A' = \begin{bmatrix} 0 & \omega_s & 0 & 0 & 0 \\ \frac{-K_1}{2H} & \frac{-D\omega_s}{2H} & \frac{-K_2}{2H} & 0 & 0 \\ \frac{-K_4}{T_{d0}} & 0 & \frac{-1}{K_3 T_{d0}} & \frac{1}{T_{d0}} & 0 \\ \frac{-K K_5}{T_A} & 0 & \frac{-K K_6}{T_A} & \frac{-1}{T_A} & 0 \\ 0 & 0 & 0 & 0 & A \end{bmatrix} \quad (18)$$

$$B' = \begin{bmatrix} 0 & 0 & 0 & 0 & B \\ 0 & 0 & 0 & 0 & 0 \end{bmatrix}^T, \quad U = \begin{bmatrix} u \\ \Delta P_d \end{bmatrix}, \quad (19)$$

$$C' = [K_5 \quad 0 \quad K_6 \quad 0 \quad C_1 C], \quad D' = [0 \quad C_2]. \quad (20)$$

## B. Numerical Optimal Control Formulation

Let the analytical model in (17), be discretized at a sample time  $t_s$ , and expressed compactly as follows:

$$x(k+1) = A_d x(k) + B_{d1} u(k) + B_{d2} \hat{d}(k) \quad (21)$$

$$\Delta V_2(k+1) = C_d x(k) + D_{d1} u(k) + D_{d2} \hat{d}(k), \quad (22)$$

and let the scheduling horizon denoted by  $\mathcal{T} = [1, \dots, T]$ . The control input should not exceed a certain limit, that is,

$$|u(k)| \leq U_{\text{lim}}, \quad \forall k \in \mathcal{T}. \quad (23)$$

Then, the voltage is required to satisfy some time restoration constraint, to enhance the performance, by introducing the TLS  $\Delta V_2(k) \models \varphi$ ,  $\forall k \in \mathcal{T}$ , where

$$\varphi = \square[(|\Delta V_2(k)| \geq \Delta V_c) \Rightarrow \diamond_{[0, t_a]} \square[(|\Delta V_2(k)| \leq \Delta V_c)]. \quad (24)$$

The above TLS states that, whenever the voltage deviation is larger than  $\Delta V_c$ , then it should become less than  $\Delta V_c$  within  $t_a$  seconds. The objective is to minimize the total control efforts, which can be represented as the summation of all decision variables as  $C_U = \sum_{k=1}^T |u(k)|$ .

The scheduling problem can be summarized as follows

$$\begin{aligned} \min \quad & C_U \quad \text{s.t.} \quad \forall k \in \mathcal{T} \\ x(k+1) &= A_d x(k) + B_{d1} u(k) + B_{d2} \hat{d}(k) \\ \Delta V_2(k+1) &= C_d x(k) + D_{d1} u(k) + D_{d2} \hat{d}(k) \\ |u(k)| &\leq U_{\text{lim}}, \\ \Delta V_2(k) &\models \varphi, \\ \varphi &= \square[(|\Delta V_2(k)| \geq \Delta V_c) \Rightarrow \diamond_{[0, t_a]} \square[(|\Delta V_2(k)| \leq \Delta V_c)]. \end{aligned} \quad (25)$$

The TLS can be encoded using the toolbox BluSTL [20]. The toolbox takes as input a linear system, a set of time constraints expressed in TLS, and a cost function. The output, is the optimized closed-loop controller, where a sequence of inputs is computed at each step, and only the first input value is used for one time step, and the process is reiterated. The approach is based on encoding the system dynamics, the TLS constraints, and the cost function together in a mixed-integer linear problem (MILP) [21], [22], written in the format of Yalmip [23], and solved by an optimization solver such as Gurobi [24].

## IV. SIMULATION AND RESULTS

The bases of the microgrid system are given as follows:

$$\begin{aligned} P_{base} &= 100 \times 10^3 \text{ [W]}, \quad V_{base} = \frac{480}{\sqrt{3}} = 391.9184 \text{ [V]}, \\ I_{base} &= \frac{P_b}{\frac{3}{2} V_b} = 170.1035 \text{ [A]}, \quad Z_{base} = \frac{V_b}{I_b} = 2.304 \text{ [ohms]}. \end{aligned}$$

The network parameters are given as follows:

$$\begin{aligned} Z_{12} &= 0.0651 + j0.1145 \text{ [p.u]}, \quad C_1 = 0.0651, \\ Y_{12} &= G_{12} + jB_{12} = \frac{1}{Z_{12}} = 3.7525 - j6.6001, \end{aligned}$$

The generator parameters are given as follows:

$$\begin{aligned} K_1 &= 3.7585, \quad K_2 = 3.6816, \quad K_3 = 0.2162, \quad K_4 = 2.6582, \\ K_5 &= 0.0544, \quad K_6 = 0.3616, \quad T_{d0} = 6s, \quad H = 4, \quad T = 0.01, \\ K &= 100, \quad D = 0. \end{aligned}$$

The parameters of the responsive model of the ESS are assumed to be  $A = -0.412$ ,  $B = -0.45$ , and  $C = 0.538$ .

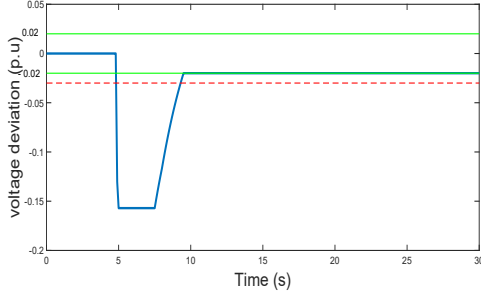


Fig. 3. Voltage deviation response for TLS (26), with  $U_{\text{lim}} = 7$ .

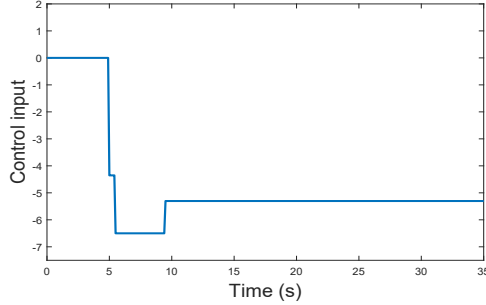


Fig. 4. Input signal for TLS (26), with  $U_{\text{lim}} = 7$ .

#### A. Case Study

Consider the state space model (17), with the above parameters, and the step disturbance  $\Delta P_d = 0.7$ . We propose to constraint the voltage deviation to satisfy the TLS formula  $\varphi = \square(\varphi_t)$ , for the scheduling problem in (25), such that,

$$\varphi_t = ((|\Delta V_2| \geq 0.02)) \Rightarrow (\diamond_{[0,5]}\square(|\Delta V_2| \leq 0.02)), \quad (26)$$

which reads “when  $|\Delta V_2|$  is larger than 0.02, it should become less than 0.02 in less than 5s for always.” This problem is simulated for two control input limits, and the simulations are illustrated in Figs. 3, 4, for  $U_{\text{lim}} = 7$ , and in Figs. 5, 6, for  $U_{\text{lim}} = 10$ . Consider now the optimal control without TLS, such that the objective is to minimize the total control effort and the voltage deviation represented as,

$$\overline{C_U} = \sum_{k=1}^T [|u(k)| + |\Delta V_2(k)|]. \quad (27)$$

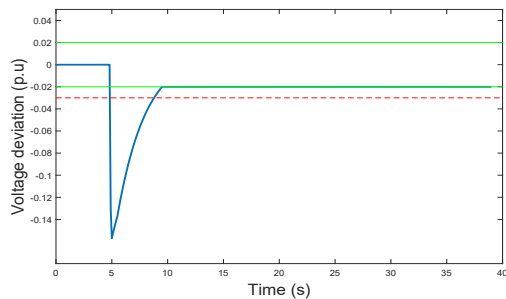


Fig. 5. Voltage deviation for TLS (26), with  $U_{\text{lim}} = 10$ .

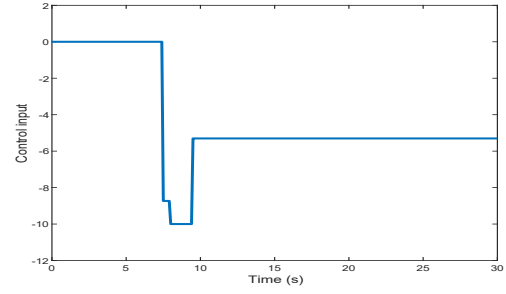


Fig. 6. Input signal for TLS (26), with  $U_{\text{lim}} = 10$ .

The scheduling problem is summarized as follows:

$$\begin{aligned} \min \quad & \overline{C_U} \quad \text{s.t.} \quad \forall k \in \mathcal{T} \\ & x(k+1) = A_d x(k) + B_{d1} u(k) + B_{d2} \hat{d}(k) \\ & \Delta V_2(k+1) = C_d x(k) + D_{d1} u(k) + D_{d2} \hat{d}(k) \\ & |u(k)| \leq U_{\text{lim}}, \\ & |u(k) - u(k-1)| \leq \Delta U_{\text{lim}}, \end{aligned} \quad (28)$$

where the rate of change constraint of the control input is added. The voltage deviation with control and without control, and the control input are simulated in Figs. 7, 8 for  $U_{\text{lim}} = 4.5$ , and in Figs. 9, 10 for  $U_{\text{lim}} = 6$ , respectively. We remark that without TLS constraint, the voltage restoration takes more than 42s for  $U_{\text{lim}} = 4.5$ . By adding more control effort, the voltage deviation will go to zero for  $U_{\text{lim}} = 6$ , but takes more than 60s. As shown, reducing the time of voltage restoration and control optimization, can be met by using TLS constraint.

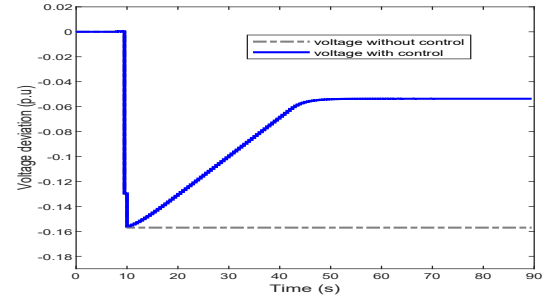


Fig. 7. Voltage deviation response without TLS, for  $U_{\text{lim}} = 4.5$ .

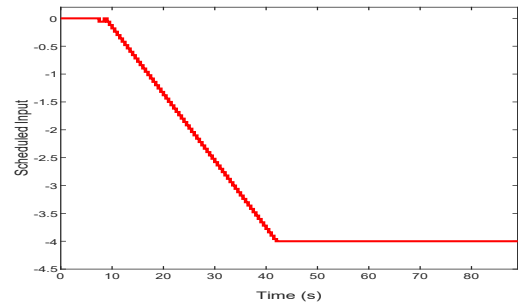


Fig. 8. Input signal without TLS, for  $U_{\text{lim}} = 4.5$ .



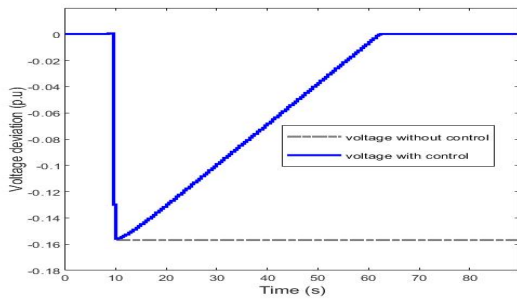


Fig. 9. Voltage deviation response without TLS, for  $U_{lim} = 6$ .

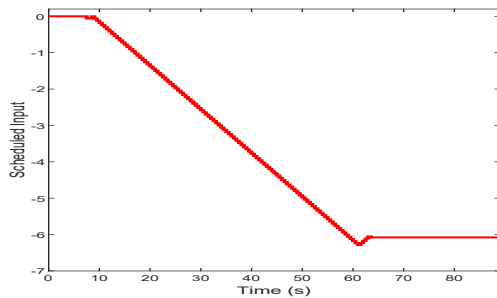


Fig. 10. Input signal without TLS, for  $U_{lim} = 6$ .

## V. CONCLUSION

In this paper, an optimal-based control scheduling approach is applied that enables the realization of voltage restoration under time constraint, by introducing the TLS. The considered model consists of a SG connected to a critical load bus. To maintain the voltage deviation, caused by a change in load demand, within set and temporal constraints simultaneously, an ESS connected to the load bus supports the voltage restoration. The reactive power input signal is obtained from a MILP, where the TLS is encoded, such that the voltage admits a specific time restoration.

## ACKNOWLEDGEMENT

Research sponsored by the Laboratory Directed Research and Development Program of Oak Ridge National Laboratory (ORNL), managed by UT-Battelle, LLC for the U.S. Department of Energy under Contract No. DE-AC05-00OR22725. By the Engineering Research Center Program of the National Science Foundation and the Department of Energy under NSF Award Number EEC-1041877 and the CURENT Industry Partnership Program.

## REFERENCES

- [1] A. Bidram and A. Davoudi, "Hierarchical structure of microgrids control system," *IEEE Transactions on Smart Grid*, vol. 4, no. 3, pp. 1963–1976, 2012.
- [2] K. Sao and W. Lehn, "Control and power management of converter fed microgrids," *IEEE Transactions on Power Systems*, vol. 3, no. 23, pp. 1088–1098, 2008.
- [3] M. Savaghebi, A. Jalilian, J. Vasquez, and J. Guerrero, "Secondary control scheme for voltage unbalance compensation in an islanded droop-controlled microgrid," *IEEE Transactions on Smart Grid*, vol. 3, no. 2, pp. 797–807, 2010.

- [4] F. Delfino, R. Pampararo, and M. Rossi, "A feedback linearization control scheme for the integration of wind energy conversion systems into distribution grids," *IEEE Systems Journal*, vol. 6, no. 1, pp. 85–93, 2012.
- [5] Z. Xu, A. A. Julius, and J. H. Chow, "Robust testing of cascading failure mitigations based on power dispatch and quick-start storage," *IEEE Systems Journal*, vol. 12, no. 4, pp. 3063–3074, 2018.
- [6] S. W. Mohod and M. V. Aware, "Micro wind power generator with battery energy storage for critical load," *IEEE Systems Journal*, vol. 6, no. 1, pp. 118–125, 2012.
- [7] A. K. Srivastava, A. A. Kumar, and N. N. Schulz, "Impact of distributed generations with energy storage devices on the electric grid," *IEEE Systems Journal*, vol. 6, no. 1, pp. 110–117, 2012.
- [8] Z. Deng, Y. Xu, H. Sun, and X. Shen, "Distributed, bounded and finite-time convergence secondary frequency control in an autonomous microgrid," *IEEE Transactions on Smart Grid*, vol. 10, no. 3, pp. 2776–2788, 2019.
- [9] S. Zuo, A. Davoudi, Y. Song, and F. L. Lewis, "Distributed finite-time voltage and frequency restoration in islanded AC microgrids," *IEEE Transactions on Industrial Electronic*, vol. 63, no. 10, pp. 5988–5997, 2016.
- [10] J. W. Simpson-Porco, Q. Shafiee, F. Dörfler, J. C. Vasquez, J. M. Guerrero, and F. Bullo, "Secondary frequency and voltage control of islanded microgrids via distributed averaging," *IEEE Transactions on Industrial Electronic*, vol. 62, no. 11, pp. 7025–7038, 2015.
- [11] A. Bidram, A. Davoudi, F. L. Lewis, and J. M. Guerrero, "Distributed co-operative secondary control of microgrids using feedback linearization," *IEEE Transactions on Power Systems*, vol. 28, no. 3, pp. 3462–3470, 2013.
- [12] Y. Zhang, M. E. Raoufat, K. Tomsovic, and S. M. Djouadi, "Set theory based safety supervisory control for wind turbines to ensure adequate frequency response," *IEEE Transactions on Power Systems*, vol. 34, no. 1, pp. 680–692, 2019.
- [13] Z. Xu, A. Julius, and J. H. Chow, "Energy storage controller synthesis for power systems with temporal logic specifications," *IEEE Syst. Journal*, vol. 13, no. 1, pp. 748–759, 2019.
- [14] —, "Coordinated control of wind turbine generator and energy storage system for frequency regulation under temporal logic specifications," in *Proc. of the Amer. Control Conf. (ACC)*, pp. 1580–1585, 2018.
- [15] Y. Zhang, M. Olama, A. Melin, Y. Xue, S. Djouadi, and K. Tomsovic, "Synthesizing distributed energy resources in microgrids with temporal logic specifications," in *Proc. of the IEEE Int. Symp. Power Electron. Distrib. Gener. Syst. (PEDG)*, pp. 1–7, 2018.
- [16] Y. Zhang, F. Taousser, M. Olamay, S. Djouadi, Y. Xuez, B. Ollisz, and K. Tomsovic, "Secondary voltage control via demand-side energy storage with temporal logic specifications," in *Proc. of the 10th Conference on Innovative Smart Grid Technologies (ISGT)*, pp. 1–5, 2019.
- [17] G. E. Fainekos and G. J. Pappas, "Robustness of temporal logic specifications for continuous-time signals," *Theoretical Computer Sciences*, vol. 410, no. 42, pp. 4262–4291, 2009.
- [18] D. Mondal, A. Chakrabarti, and A. Sengupta, *Power System Small Signal Stability Analysis and Control*. Elsevier, 2014.
- [19] D. N. Trakas and N. D. Hatziargyriou, "Optimal distribution system operation for enhancing resilience against wildfires," *IEEE Transactions on Power Systems*, vol. 33, no. 2, pp. 2260–2271, 2018.
- [20] A. Donzé, V. Raman, G. Frehse, and M. Althoff, "Blustl: Controller synthesis from signal temporal logic specifications," in *Proc. of the 1st and 2nd International Workshop on Applied Verification for Continuous and Hybrid Systems*, pp. 160–168, 2015.
- [21] V. Raman, A. Donze, D. Sadigh, R. Murray, and S. A. Seshia, "Reactive synthesis from signal temporal logic specifications," in *Proc. of the International Conference on Hybrid Systems: Computation and Control (HSCC)*, pp. 226–227, 2015.
- [22] V. Raman, M. Maasoumy, A. Donze, R. Murray, A. Sangiovanni-Vincentelli, and S. A. Seshia, "Model predictive control with signal temporal logic specifications," in *Proc. of the IEEE Conf. on Decision and Control (CDC)*, pp. 215–243, 2014.
- [23] J. Löfberg, "YALMIP: A toolbox for modeling and optimization in MATLAB," in *Proc. of the IEEE CCA/SIC/CACSD Conf.*, 2004. [Online]. Available: <http://users.isy.liu.se/johanl/yalmip/>
- [24] *Gurobi Optimizer*, Gurobi ApS, 2018. [Online]. Available: [http://www.gurobi.com/documentation/8.0/quickstart\\_windows.pdf](http://www.gurobi.com/documentation/8.0/quickstart_windows.pdf)